FLOW AND HEAT TRANSFER OF MHD GRAPHENE OXIDE-WATER NANOFLUID BETWEEN TWO NON-PARALLEL WALLS

by

Mohammadreza AZIMI and Rouzbeh RIAZI *

Faculty of New Sciences and Technologies, University of Tehran, Tehran, Iran

Original scientific paper
https://doi.org/10.2298/TSCI150513100A

The steady 2-D heat transfer and flow between two non-parallel walls of a graphene oxide nanofluid in presence of uniform magnetic field are investigated in this paper. The analytical solution of the non-linear problem is obtained by Galerkin optimal homotopy asymptotic method. At first a similarity transformation is used to reduce the partial differential equations modeling the flow and heat transfer to ordinary non-linear differential equation systems containing the semi angle between the plate's parameter, Reynolds number, the magnetic field strength, nanoparticle volume fraction, Eckert and Prandtl numbers. Finally, the obtained analytical results have been compared with results achieved from previous works in some cases.

Key words: *heat transfer enhancement, graphene oxide-water, nanofluid, Jeffery-Hamel flow, Galerkin optimal homotopy asymptotic method*

Introduction

The term nanofluid was envisioned to describe a fluid in which nanometer sized particles were suspended in conventional heat transfer basic fluids. Nanotechnology aims to manipulate the structure of the matter at the molecular level with the goal for innovation in virtually every industry and public endeavor including biological sciences, physical sciences, electronics cooling, transportation, the environment, and national security [1, 2].

The MHD is the study of the interaction of electrically conducting fluids and electromagnetic forces. The field of MHD was initiated by Swedish physicist, Alfven [3] for which he received in 1970 the Nobel Prize. The official birth of incompressible fluid MHD is 1936-1937. In 1937, Hartmann [4] studied the influence of a transverse uniform magnetic field on the flow of a viscous incompressible electrically conducting fluid between two infinite parallel stationary and insulating plates.

Graphene was found to display high quality electron transport at room temperature. Theoretical study was performed on determination of thermal conductivity of graphene and suggests that it has unusual thermal conductivity [5].

Rashidi *et al*. [6] considered the analysis of the second law of thermodynamics applied to an electrically conducting incompressible nanofluid fluid flowing over a porous rotating disk. They concluded that using magnetic rotating disk drives has important applications in heat transfer enhancement in renewable energy systems. Ellahi [7] studied the MHD flow of non-Newtonian nanofluid in a pipe. He observed that the MHD parameter decreases the fluid motion and the velocity profile is larger than that of temperature profile even in the presence of variable viscosities.

* Corresponding author, e-mail: ro_riazi@ut.ac.ir

Sheikholeslami and Abelman [8] used two phase simulation of nanofluid flow and heat transfer in an annulus in the presence of an axial magnetic field. Sheikholeslami and Rashidi [9] studied the effect space dependent magnetic field on free convection of Fe_3O_4-water nanofluid. They showed that Nusselt number decreases with increase of Lorentz forces. Sheikholeslami *et al*. [10] applied the lattice Boltzmann method to simulate 3-D nanofluid flow and heat transfer in presence of magnetic field. They indicated that adding magnetic field leads to decrease in rate of heat transfer. Sheikholeslami [11] studied the effect of spatially variable magnetic field on ferrofluid flow and heat transfer considering constant heat flux boundary condition. He found that enhancement in heat transfer decreases with increase of Rayleigh number and magnetic number but it increases with increase of Hartmann number. Theoretical study of steady-flow of an electrically conducting fluid in channels of varying width finds applications in engineering and biological systems, *e. g*. control of liquid metal flows, crystal growth, design of medical diagnostic devices which make use of the interaction of magnetic fields with tissue fluids, *etc.* [12].

The incompressible viscous fluid flow through convergent and divergent channels is one of the most applicable cases in fluid mechanics, electrical, and biomechanical engineering. One of the most significant examples of Jeffery-Hamel problems are those subjected to an applied magnetic field. The MHD systems are used effectively in many applications including power generators, pumps, accelerators, electrostatic filters, droplet filters, the design of heat exchangers, the cooling of reactors, *etc*. The investigation on MHD fluid flow was the main purpose of many pervious researches [13, 14].

In the heart of all the different engineering sciences, everything shows itself in the mathematical relation that most of these problems and phenomena are modeled by ordinary or partial differential equations. In most cases, scientific problems are inherently of non-linearity that does not admit exact solution, so these equations should be solved using special techniques. Some of these methods are homotopy perturbation method [15], reconstruction of variational iteration method [16], Glerkin optimal homotopy asymptotic method (GOHAM) [17], and others [18, 19].

The aim of this study is to investigate the velocity profile in MHD Jeffery-Hamel flow with nanoparticles by using GOHAM. The obtained approximate result will be compared to numerical solution in numerical case.

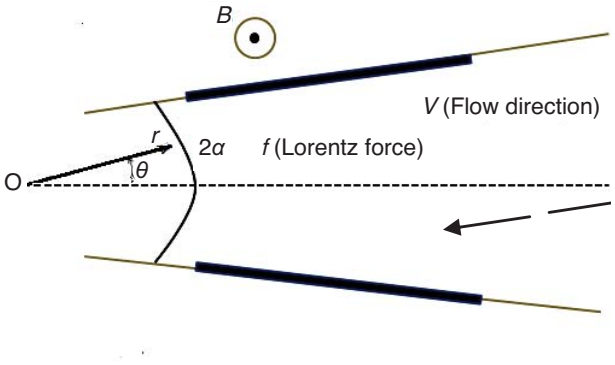

Figure 1. Geometry of the problem

Mathematical formulation

For an analytical study of Jeffery-Hamel MHD flows, we consider the 2-D flow of a viscous, incompressible and electrically conducting fluid in the presence of a homogeneous magnetic field which acts transversely to the flow fig. 1.

As it can be seen in fig. 1 the steady 2-D flow of an incompressible conducting viscous fluid from a source or sink at the intersection between two non-parallel plane walls is considered.

We assume that the velocity is purely radial and depends on r and θ only. The mass, momentum, and energy equations in polar co-ordinates are:

$$\frac{\rho_{\mathrm{nf}}}{r}\frac{\partial\left[ru(r,\theta)\right]}{\partial r}\left[ru(r,\theta)\right]=0 \tag{1}$$

$$u(r,\theta)\frac{\partial u(r,\theta)}{\partial r}=\nu_{\mathrm{nf}}\left[\frac{\partial^2 u(r,\theta)}{\partial r^2}+\frac{1}{r}\frac{\partial u(r,\theta)}{\partial r}+\frac{1}{r^2}\frac{\partial^2 u(r,\theta)}{\partial\theta^2}-\frac{u(r,\theta)}{r^2}\right]-\frac{1}{\rho_{\mathrm{nf}}}\frac{\partial P}{\partial r}-\frac{\sigma B_0^2}{\rho_{\mathrm{nf}}r^2}u(r,\theta)a \tag{2}$$

$$-\frac{1}{\rho_{\mathrm{nf}}r}\frac{\partial P}{\partial\theta}+\frac{2\mu_{\mathrm{nf}}}{\rho_{\mathrm{nf}}r^2}\frac{\partial u(r,\theta)}{\partial\theta}=0 \tag{3}$$

$$u(r,\theta)\frac{\partial T(r,\theta)}{\partial r}=\alpha_{\mathrm{nf}}\left[\frac{\partial^2 T(r,\theta)}{\partial r^2}+\frac{1}{r}\frac{\partial T(r,\theta)}{\partial r}+\frac{1}{r^2}\frac{\partial^2 T(r,\theta)}{\partial\theta^2}\right]+$$

$$+\frac{\mu_{\mathrm{nf}}}{\left(\rho C_p\right)_{\mathrm{nf}}}\left\{4\left[\frac{\partial u(r,\theta)}{\partial r}\right]+\frac{1}{r^2}\left[\frac{\partial u(r,\theta)}{\partial\theta}\right]^2\right\} \tag{4}$$

Since we have a symmetric geometry, the boundary conditions will be:

$$\begin{gathered}\frac{\partial u(r,\theta)}{\partial r}=0,\ \ \frac{\partial T(r,\theta)}{\partial\theta}=0,\ \ u(r,\theta)=0 \qquad \text{at the channel centerline}\\ T=T_w,\ \ u(r,\theta)=0 \qquad \text{at the plates}\end{gathered} \tag{5}$$

where B_0 is the electromagnetic induction, $u(r)$ – the velocity along radial direction, P – the fluid pressure, σ – the conductivity of the fluid, ρ_{nf} – the density of fluid, and υ_{nf} – the coefficient of kinematic viscosity. By introducing φ as a solid volume fraction, fluid density, dynamic viscosity, the kinematic viscosity [16], thermal diffusivity and thermal conductivity [17] of nanofluid can be written:

$$\left.\begin{aligned}\rho_{\mathrm{nf}}&=\rho_f(1-\varphi)+\rho_s\varphi\\ \mu_{\mathrm{nf}}&=\frac{\mu_f}{(1-\varphi)^{2.5}}\\ \nu_{\mathrm{nf}}&=\frac{\mu_f}{\rho_{\mathrm{nf}}}\\ \alpha_{\mathrm{nf}}&=\frac{k_{\mathrm{nf}}}{\left(\rho C_p\right)_{\mathrm{nf}}}\\ \frac{k_{\mathrm{nf}}}{k_f}&=\frac{\left(k_s+2k_f\right)-2\varphi\left(k_s-k_f\right)}{\left(k_s+2k_f\right)+\varphi\left(k_s-k_f\right)}\end{aligned}\right\} \tag{6}$$

Using $\eta=\theta/\alpha$ as the semi angle between walls, the dimensionless form of the velocity parameter can be yield by dividing that to its maximum values as $f(\eta)=f(\theta)/f_{\max}$ where $f_{max}=rU$. Introducing $\zeta=T/T_w$, substituting dimensionless parameters into eqs. (1)-(5) and eliminating the pressure term implies the following non-linear third order boundary value problems:

$$f'''+2\alpha\,\mathrm{Re}\left\{\left[(1-\varphi)+\frac{\rho_s}{\rho_f}\varphi\right](1-\varphi)^{2.5}\right\}ff'+\left[4-(1-\varphi)^{1.25}\,\mathrm{Ha}\right]\alpha^2 f'=0 \tag{7}$$

$$\frac{1}{1-\varphi+\varphi\dfrac{\left(\rho C_p\right)_s}{\left(\rho C_p\right)_f}}\left[\frac{k_{\mathrm{nf}}}{k_f}\zeta''+\frac{\mathrm{Pr\,Ec}}{\left(1-\varphi\right)^{2.5}}\left(4\alpha^2 f^2+f'^2\right)\right]=0 \tag{8}$$

where $\mathrm{Pr} = [\mu_f\ (C_p)_f] / k_f$ is the Prandtl number, $\mathrm{Re} = \alpha U_{max} / \nu$ is a Reynolds number, $\mathrm{Ec} = U^2 / (C_p)_f T_w$ is Eckert number, and $\mathrm{Ha} = (\sigma B_0{}^2 / \rho\upsilon)^{1/2}$ is the Hartmann number.

With the following boundary conditions:

$$f(0)=1,\quad f(1)=0,\quad f'(0)=0,\quad \zeta(1)=1,\quad \zeta'(0)=0 \tag{9}$$

In the limit of $\alpha = 0$, the flow becomes that of plane Poiseuille flow between two parallel plates. Physical quantities of interest are the skin friction coefficient, local Nusselt number, heat transfer rate, and shear stress which are defined:

$$c_f=\frac{\tau_w}{\rho_f U^2},\quad \mathrm{Nu}=\frac{r\,q_w\big|_{\theta=\alpha}}{k_f T_w},\quad q_w=-k_{\mathrm{nf}}\nabla T,\quad \tau_w=\mu_{\mathrm{nf}}\left\{\frac{1}{r}\left[\frac{\partial u(r,\theta)}{\partial\theta}\right]\right\} \tag{10}$$

substitution of eq. (10) into eqs. (7)-(8), gives:

$$c_f=\frac{1}{\mathrm{Re}\left(1-\varphi\right)^{2.5}}f'(1),\quad \mathrm{Nu}=-\frac{1}{\alpha}\frac{k_{\mathrm{nf}}}{k_f}\zeta'(1) \tag{11}$$

Application of GOHAM

Following differential equation is considered:

$$L\left[u(t)\right]+N\left[u(t)\right]+g(t)=0,\quad B(u)=0 \tag{12}$$

where L is a linear operator, $u(t)$ – an unknown function, $g(t)$ – a known function, $N[u(t)]$ – a non-linear operator, and B – a boundary operator. By means of OHAM one first constructs a set of equations:

$$(1-p)\left\{L\left[\phi(\tau,p)+g(\tau)\right]\right\}-H(p)\left\{L\left[\phi(\tau,p)\right]+g(\tau)+N\left[\phi(\tau,p)\right]\right\}B\left[\phi(\tau,p)\right]=0 \tag{13}$$

where τ is an independent variable, $p \in [0.1]$ – an embedding parameter, $H(p)$ denotes a non-zero auxiliary function for $p \neq 0$ and $H(0) = 0$, and $\phi(\tau, \rho)$ is an unknown function. Obviously, when $p = 0$ and $p = 1$, it holds that:

$$\phi(\tau,0)=u_0(\tau),\quad \phi(\tau,1)=u(\tau) \tag{14}$$

Thus, as p increases from 0 to 1, the solution $\phi(\tau, \rho)$ varies from $u_0(\tau)$ to the solution $u(\tau)$, where $u_0(\tau)$ is obtained from eq. (14) for $p = 0$:

$$L\left[u_0(\tau)\right]+g(\tau)=0,\quad B(u_0)=0 \tag{15}$$

The auxiliary function $H(p)$ can be chosen in the form:

$$H(p)=p_1C_1+p_2C_2+\cdots \tag{16}$$

where C_1, C_2, ... are constants which can be determined later. Expanding $\phi(\tau, \rho)$ in a series with respect to p, one has:

$$\phi(\tau, p, C_i) = u_0(\tau) + \sum_{k>1} u_k(\tau, C_i) p_k, \quad i = 1, 2, \ldots \tag{17}$$

Substituting eq. (16) into eq. (13), collecting the same powers of p, and equating each coefficient of p to zero, we obtain set of differential equation with boundary conditions. Solving differential equations by boundary conditions $u_0(\tau)$, $u_1(\tau, C_1)$, $u_2(\tau, C_2)$, ... are obtained. Generally speaking, the solution of eqs. (7) and (8) can be determined approximately in the form:

$$\phi(\tau, p, C_i) = u_0(\tau) + \sum_{k>1} u_k(\tau, C_i) p_k, \quad i = 1, 2, \ldots \tag{18}$$

$$\tilde{u}(m) = u_0(\tau) + \sum_{k=1}^{m} u_k(\tau, C_i) \tag{19}$$

Note that the last coefficient C_m can be function of τ. Substituting eq. (19) into eq. (12), there results the following residual:

$$R(\tau, C_i) = L\left[\tilde{u}^{(m)}(\tau, C_i)\right] + g(\tau) + N\left[\tilde{u}^{(m)}(\tau, C_i)\right] \tag{20}$$

If $R(\tau, C_i) = 0$ then $\tilde{u}^{(m)}(\tau, C_i)$ happens to be the exact solution. Generally such a case will not arise for non-linear problems, but the functional by Galerkin method can be minimized:

$$w_i = \frac{\partial R(\tau, C_1, C_2, \cdots, C_m)}{\partial C_i}, \quad i = 1, 2, \ldots, m \tag{21}$$

The unknown constants $C_i (i = 1, 2, \ldots, m)$ can be identified from the conditions:

$$J(C_1, C_2) = \int_a^b w_i R(\tau, C_1, C_2, \ldots, C_m) \, \mathrm{d}\tau = 0 \tag{22}$$

where a and b are two values, depending on the given problem. With these constants, the approximate solution (of order m) eq. (22) is well determined. It can be observed that the method proposed in this work generalizes these two methods using the special (more general) auxiliary function $H(p)$.

Results and discussions

The problem of MHD flow of nanofluid is associated with various kinds of dimensionless parameters due to its multi-physics nature. In this section, we will also discuss about the obtained results of graphene oxide (GO)-water nanofluid flow between converging-diverging plates for various solid volume fraction, Eckert, Reynolds, and Hartman numbers. The physical properties of GO-water nanofluid are tabulated in tab. 1.

Figure 2(a) shows the effect of increasing Reynolds numbers on the fluid velocity for fixed Hartmann numbers when $\alpha = \pi/9$, $\phi = 0.2$, Ha = 300. As it can be illustrated in fig. 2(a) back flow is possible for large Reynolds numbers in the case of diverging channels. The effect of Hartmann number for a diverging channel is demonstrated in fig. 2(b). The velocity curves show that the rate of momentum transport is considerably reduced with increase of Hartmann number.

Table 1. Thermophysical properties of water and GO-water nanoparticle [16].

	ρ [kgm^{-3}]	C_p [Jkg^{-1}k^{-1}]	k [Wm^{-1}k^{-1}]
Pure water	997.1	4179	0.613
GO-water	1800	717	5000

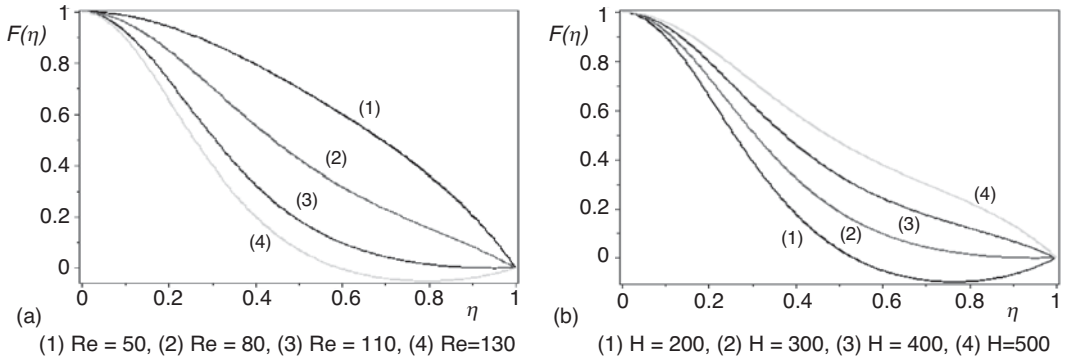

Figure 2. Effect of Reynolds and Hartmann numbers on velocity profile when $\alpha = \pi / 9$, $\varphi = 0.2$, (a) Ha = 300 and (b) Re = 110

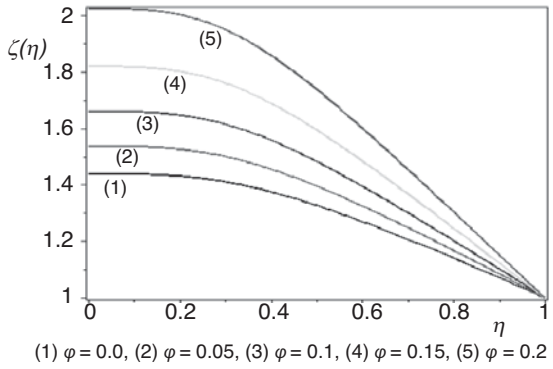

Figure 3. Effect of Nanoparticle solid volume fraction on temperature profile in case Ha = 400, Re = 110, Ec = 0.2, Pr = 7, and $\alpha = \pi / 12$

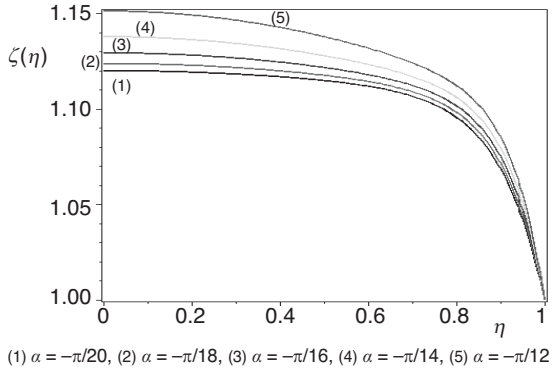

Figure 4. Effect of angle between plates on temperature profile when Ha = 100, Re = 70, Ec = 0.1, Pr = 7, and $\varphi = 0.1$ for converging channel

This clearly indicates that the transverse magnetic field opposes the transport phenomena. Because the that variation of Hartmann number leads to the variation of the Lorentz force due to magnetic field and the Lorentz force produces more resistance to transport phenomena.

Nanosolid volume fraction plays key role and it has significant effect on both velocity and temperature components. Figure 3 illustrates the effect of solid volume fraction of GO nanoparticle on temperature profile in case Ha = 400, Re = 110, Ec = 0.2, Pr = 7, and $\alpha = \pi / 12$.

The increase in GO-nanoparticles volume fraction tends to increase the dimensionless temperatures due to increase in heat transfer. For energy applications of nanofluids, two remarkable properties of nanofluids are utilized, one is the higher thermal conductivities of nanofluids, enhancing the heat transfer, and another is the absorption properties of nanofluids. In this study, the absorption properties of GO-water nanofluid are considered negligible.

The effect of semi angle between non-parallel walls on non-dimensional temperature of the nanofluid is investigated through fig. 4 for convergent channel when the other non-dimensional parameters are kept fixed in Ha = 300, Re = 70, Ec = 0.1, Pr = 7, and $\varphi = 0.1$.

This figure describe that the temperature is increasing function of α in convergent channels.

The effect of semi angle between non-parallel walls on velocity profile of the nanofluid is investigated through figs. 5(a) and 5(b) for both convergent and divergent channel in case $\varphi = 0.2$, Ha = 400, and Re = 50.

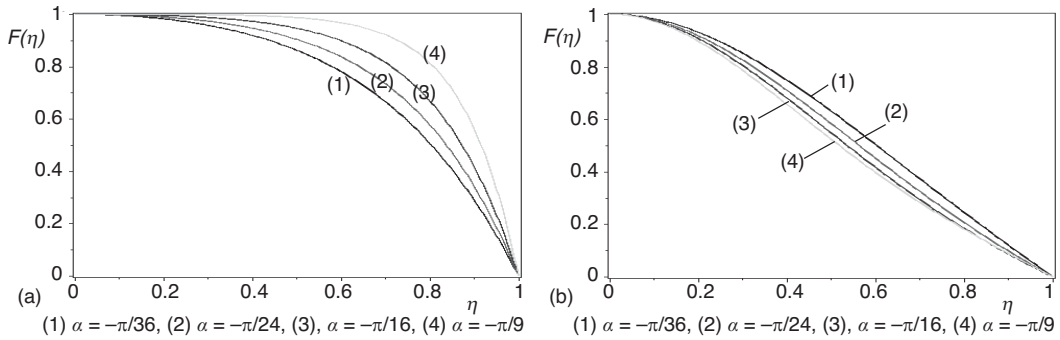

Figure 5. Effect of semi angle between walls on velocity profile when $\varphi = 0.2$, Ha = 400 and Re = 50 (a) convergent channel and (b) divergent channel

Impact of Eckert number and Hartmann number on temperature profiles are display in figs. 6(a) and 6(b), respectively. Figure 5 confirm that when Eckert number increases, temperature profiles increase whereas increasing Hartmann number reduces velocity values. This is in line with the physics of the system in that because of the higher thermal conductivity at higher Eckert numbers, higher values of thermal diffusivity can be observed.

Another consequence which can be achieved from fig. 6 is that, by changing the value of Hartmann number from 100 to 200, temperature on wall is decreased from 1.18 to 1.13. Such an effect even becomes less sensible at higher values of Hartman number. Also, it shows that increasing Eckert number leads to increasing the curve of presented surface when Hartman number is constant.

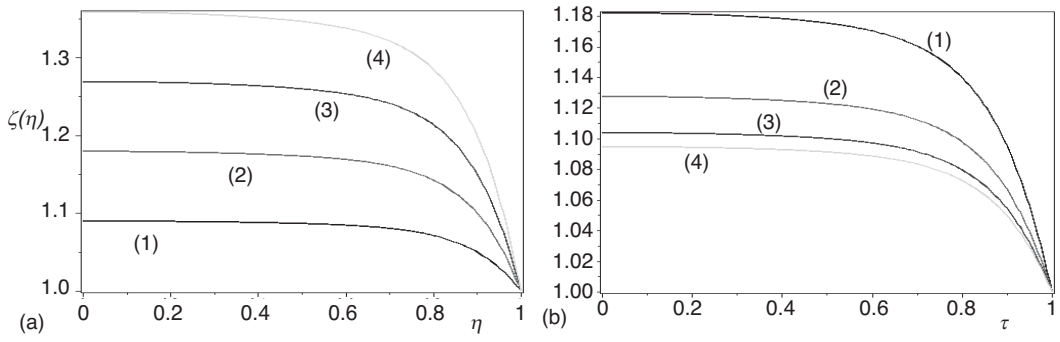

Figure 6. Effect of Eckert and Hartmann numbers on temperature profile when $\alpha = -\pi / 24$, Re = 70, Pr = 7, $\varphi = 0.1$, (a) Ha = 400 and (b) Ec = 0.05

The variations in the skin friction coefficient and the Nusselt number with the governing parameters are presented in tabs. 2 and 3, respectively. According to the performed calculations in eq. (5) and tab. 2, one can thoroughly consider that generally, adding nanoparticles to the working fluid results in an increase in the value of Nusselt number. By increasing the value of nanoparticles volume fraction, the heat transfer rate raises.

Table 2. Nusselt number in case Ha = 50 and $\alpha = 15^o$

Solid volume fraction	Ec	Re	Nu
0.1	0.1	50	4.9010
0.2			7.0706
0.1	0.2		9.8024
0.2			14.141
0.1	0.1	100	9.4166
0.2			13.8571
0.1	0.2		18.8331
0.2			27.713

Effects of angle of the channel, Reynolds number and Hartmann number on skin friction coefficient is shown in tab. 3. Skin friction coefficient is an increasing function of Reynolds number and opening angle but decease function of Hartmann number.

Interestingly, it is not clearly evident to out rightly predict the effects of the different Eckert number values on Nusselt number. This may be because of the complications of the proposed model. Nevertheless, the present study provided a good base for further research.

Table 4 shows a comparison between GOHAM solution and ADM solution [20] for velocity when Ha = 250, Re = 25, $\alpha = 5$, and $\phi = 0$.

Table 3. Skin friction coefficient in case $\varphi = 0.15$

Angle between plates	Ha	Re	Skin friction coefficient
5^o	50	25	–0.1771
10^o			–0.2173
5^o	100		–0.1802
10^o			–0.2282
5^o	50	50	–0.1049
10^o			–0.1377
5^o	100		–0.1063
10^o			–0.1424

Table 4. Comparison between DTM solution and ADM solution [20] when Ha = 250, Re = 25, $\alpha = 5$, $\varphi = 0$

η	GOHAM	ADM [14]	Error
0	1.000000	1.000000	0.000
0.2	0.954700	0.960841	0.007
0.4	0.821345	0.811225	0.012
0.6	0.614891	0.604866	0.009
0.8	0.339890	0.325834	0.014
1	0.000000	0.000000	0.000

Conclusions

This investigation deals with the analysis of heat transfer and MHD viscous GO-water nanofluid flow between two non-parallel walls for both converging/diverging cases.

Based on achieved results, an increase in the magnetic field intensity was found to have a strong stabilizing effect on the results for both diverging and converging channel geometries.

The results show that the non-dimensional parameters have a strong influence on the temperature profile. The main findings are summarized as follows.

- The thickness of thermal boundary layer decreases with increment in solid volume fraction of nanofluid due to higher heat transfer.
- Nusselt number is an increasing function of Reynolds number, solid volume fraction and Eckert number.

- Skin friction coefficient is an increasing function of Reynolds number and opening angle but decease function of Hartmann number.
- The comparison between analytical results and results achieved by previous researches revealed that GOHAM can be simple, powerful and efficient techniques for finding analytical solutions in science and engineering non-linear differential equations.

Nomenclature

B_0 – magnetic field, [Wbm^{-2}]
Ec – Eckert number
$f(\eta)$ – dimensionless velocity
Ha – Hartmann number
P – pressure term
Pr – Prandtl number
Re – Reynolds number
r, θ – cylindrical co-ordinates
T – temperature, [K]
T_w – wall temperature, [K]
U_{max} – maximum value of velocity, [ms^{-1}]
u, v – velocity components along x-, y- axes, respectively

Greek symbols

α – angle of the channel
η – dimensionless angle
θ – any angle
ρ – density, [kgm^{-3}]
μ – dynamic viscosity, [kgm^{-1}s^{-1}]
ν – kinematic viscosity, [m^{2}s^{-1}]
φ – nanoparticle volume fraction
ζ – dimensionless temperature

Subscripts

nf – nanofluid
f – base fluid
s – nano-solid-particles

References

[1] Mahian, O., *et al*., A Review of the Applications of Nanofluids in Solar Energy, *Int. J. Heat Mass Transfer*, *57* (2013), 2, pp. 582-594
[2] Cimpean, D. S., Pop, I., Fully Developed Mixed Convection Flow of a Nanofluid through an Inclined Channel Filled with a Porous Medium, *Int. J. Heat Mass Transfer*, *55* (2012), 4, pp. 907-914
[3] Alfven, H., Existence of Electromagnetic-Hydrodynamic Waves, *Nature*, *150* (1942), 3805, pp. 405-406
[4] Hartmann, J., *Hg-Dynamics I: Theory of the Laminar Flow of an Electrically Conducting Liquid in a Homogeneous Magnetic Field*, Levin & Munksgaard, Ejnar Munksgaard, Copenhagen, 1937
[5] Saito, K., *et al*., Ballistic Thermal Conductance of a Graphene Sheet, *Phys. Rev. B: Condens Matter*, *76,* (2007), ID 115409
[6] Rashidi, M. M., *et al*., Entropy Generation in Steady MHD Flow Due to a Rotating Porous Disk in a Nanofluid, *Int. J. Heat Mass Transfer*, *62* (2013), July, pp. 515-525
[7] Ellahi, R., The Effects of MHD and Temperature Dependent Viscosity on the Flow of Non-Newtonian Nanofluid in a Pipe: Analytical Solutions, *Appl. Math. Model., 37* (2013), 3, pp. 1451-1467
[8] Sheikholeslami, M., Abelman, S., Two Phase Simulation of Nanofluid Flow and Heat Transfer in an Annulus in the Presence of an Axial Magnetic Field, *IEEE Transactions on Nanotechnology*, *14* (2015), 3, pp. 561-568
[9] Sheikholeslami, M., Rashidi, M. M., Effect of Space Dependent Magnetic Field on Free Convection of Fe_3O_4-Water Nanofluid, *J. Taiwan. Inst. Chem., E*, *56* (2015), Nov., pp. 6-15
[10] Sheikholeslami, M., *et al*., Lattice Boltzmann Method for Simulation of Magnetic Field Effect on Hydrothermal Behavior of Nanofluid in a Cubic Cavity, *Physica A: Statistical Mechanics and its Applications*, *432* (2015), Aug., pp. 58-70
[11] Sheikholeslami, M., Effect of Spatially Variable Magnetic Field on Ferrofluid Flow and Heat Transfer Considering Constant Heat Flux Boundary Condition, *Eur. Phys. J. Plus., 129* (2014), Nov., pp. 248-260
[12] Sheikholeslami, M., *et al*., Investigation of Nanofluid Flow and Heat Transfer in Presence of Magnetic Field Using KKL Model, *Arab. J. Sci. Eng., 39* (2014), 6, pp. 5007-5016
[13] Raftari, B., Yildirim, A., The Application of Homotopy Perturbation Method for MHD Flows of UCM Fluids above Porous Stretching Sheets, *Comp. Math. Appl., 59* (2010), 10, pp. 3328-3337
[14] Ganji, D. D., Azimi, M., Application of DTM on MHD Jeffery Hamel Problem with Nanoparticles, *U.P.B. Scientific Bulletin: D*, *75* (2013), 1, pp. 223-230
[15] Ganji, D. D., *et al*., Determination of Temperature Distribution for Annular Fins with Temperature Dependent Thermal Conductivity by HPM*, Thermal Science, 15* (2011), 1, pp. 111-115

[16] Azimi, A., Azimi, M., Analytical Investigation on 2-D Unsteady MHD Viscoelastic Flow between Moving Parallel Plates Using RVIM and HPM, *Walailak J. Sci. & Tech., 11* (2014), 11, pp. 955-963
[17] Azimi, M., *et al.,* Investigation of the Unsteady Graphene Oxide Nanofluid Flow between Two Moving Plates, *J. Comput. Theor. NanoScie., 11* (2014), 10, pp. 2104-2108
[18] Ganji, D. D., Azimi, M., Application of Max Min Approach and Amplitude Frequency Formulation to the Nonlinear Oscillation Systems, *U.P.B. Scientific Bulletin: A, 74* (2012), 3, pp. 131-140
[19] Ganji, D. D., *et al.,* Energy Balance Method and Amplitude Frequency Formulation Based of Strongly Nonlinear Oscillator, *Indian J. Pure Ap. Mat., 50* (2012), 9, pp. 670-675
[20] Sheikholeslami, M., *et al*., Analytical Investigation of Jeffery Hamel Flow with High Magnetic Field and Nanoparticle by Adomian Decomposition Method, *App. Math Mech.-Engl., 33* (2012), 1, pp. 25-36

Paper submitted: May 13, 2015
Paper revised: June 19, 2015
Paper accepted: July 1, 2015